Hindawi Publishing Corporation
Journal of Nanomaterials
Volume 2010, Article ID 403197, 5 pages
doi:10.1155/2010/403197

Research Article

Effects of Current on Arc Fabrication of Cu Nanoparticles

M. Z. Kassaee,[1] F. Buazar,[2] and E. Motamedi[1]

[1] *Department of Chemistry, Tarbiat Modares University, P.O. Box 14115-175, Tehran, Iran*
[2] *Department of Marine Chemistry, Khoramshahr Marine Science and Technology University, P.O. Box 669, Khoramshahr, Iran*

Correspondence should be addressed to M. Z. Kassaee, kassaeem@modares.ac.ir and F. Buazar, buazar@modares.ac.ir

Received 3 May 2009; Revised 17 August 2009; Accepted 8 January 2010

Academic Editor: Lian Gao

Arc-fabricated copper nanoparticles (Cu Nps) size, morphology and the crystalline structure, as well as the yields of Nps appear sensitive to the applied currents (50–160 A) in distilled water. The results indicate that the sizes of Cu Nps are directly proportional to the currents employed. At 50 A, TEM, XRD, and SEM analyses show fabrication of relatively purest, the most dispersed, face-centered cubic (fcc) brown Cu Nps with rather smallest average size of 20 nm. At the same current, the TGA-DTA analysis reveals neither weight loss nor gain, indicating thermal stability of the fabricated Cu Nps.

1. Introduction

There is a significant interest in the syntheses and applications of nanoparticles (Nps) [1]. Following the great implications of copper for its high electrical conductivity and catalytic properties, copper nanoparticles (Cu Nps) are now attracting great technological interests [2–4]. Many techniques are developed to prepare copper nanostructures, including ultrasonic-chemical [5], electrolysis [6], sol-gel [7], inverse microemulsion [8], chemical reduction [9], microwave irradiation [10], supercritical extraction [11], hydrothermal method [12], laser ablation [13], plasma [14], and submerged arc nanoparticle synthesis system (SANSS) [15–21]. Among these methods, electric arc evaporation is the most efficient method for the direct fabrication of Cu Nps (one-pot synthesis) through formation of dense metal-vapor-clouds. The latter formed because of the high temperature and compactness of the electrode spots produced as the arc attachment points [14]. Formation of uniform CuO nanorods along with CuO, Cu_2O, and Cu Nps *via* a solid-liquid phase arc discharge process is reported [22]. Also, Cu Nps and Cu nanofluid fabrication through a pressure control technique called "arc-submerged nanoparticle synthesis system (ASNSS)" is reported by Tsung et al. [15, 16]. Consequently, they used SANSS to prepare CuO Nps dispersed uniformly in dielectric liquid [17–21], and also they fabricated Ag, Ni, and TiO_2 using this method [23–25]. We have also reported syntheses of the low-cost Cu Nps and Cu_2O Nps preparation through explosion of copper wires [26]. Water introduced as the medium of choice by many reports, including our recent account of media effects on arc fabrications of nanobrass (63%Cu + 37%Zn) [27]. While arc fabrication of Cu Nps in distilled water is already reported, the crucial role of current is not addressed yet. Hence, in this manuscript we adopt distilled water for probing the effects of current (50–160 A) on the arc fabrications of Cu Nps. It is found that density of current is a key factor for the morphology, controlling particle sizes, and yields of copper Nps. Increasing the current can cause to increasing the particle sizes and decreasing the yield of Nps production [28].

2. Experimental

Our arc method requires only a direct current (DC) power supply and commercially available copper rods. Two high-purity copper rods (95.90%) with diameters of 2.5 mm and length of 30 mm are employed as a movable anode and a static cathode in our arc discharge experiments in distilled water. The distance between the two copper electrodes is set at 1 mm with a 45° angle between the two electrodes. Different currents (30, 50, 70, 90, 100, 115, 150, 160 amperes) are passed through water-submerged copper electrodes (1–10 milliseconds). The arc discharge is

initiated by slowly detaching the moveable anode from the cathode. Consequently, the cathode-anode gap is controlled at approximately 1 mm to maintain a stable discharge current and average voltage of 25 V in experiments. Separating the electrodes increases the voltage, while bringing the electrodes close together decreases it. The voltages and currents employed are recorded when stable discharge conditions are attained.

The Cu electrodes are heated by the high temperature of the arc, and metal atoms are separated from the metal surface and evaporated into metal vapour. The cooled metal vapor in water lead to the formation of primary particles by nucleation mechanism turning into Cu Nps dispersed in distilled water [29]. Gas bubbles are formed in the water during the arc process due to the plasma vaporization/decomposition of the anode material and water. These escaping gas bubbles act both as a condensing media and as carriers of the final products to the water surface. The growth rate of the nucleus is controlled by the concentration of the vaporized metal and the temperature of the medium [30]. The X-ray powder diffraction (XRD), scanning electron microscopy (SEM), and transmission electron microscopy (TEM) are used for depiction crystalline structure, morphology, and size of Cu Nps, respectively. Thermal stability of Cu Nps is characterized by thermogravimetric and differential thermal analyses (TGA-DTA).

3. Results and Discussion

Our objective in this work is to find the best current for fabrication Cu Nps with the better uniformity, good particle size distribution, and the higher yield. We discussed in detail the impact of current on the metal Nps fabrication elsewhere [28]. Eight different currents (30, 50, 70, 90, 100, 115, 150, and 160 A) are passed through Cu electrodes. At the employed currents ≥50 A, two distinct nanopowders (*w/w* 50 : 1) are obtained which become easily separated through filtration. The major nanopowder is a brown precipitate which consists of pure Cu Nps, while the minor product is a black color, water-suspended mixture of Nps, consisting of copper oxide Nps (CuO and Cu_2O Nps).

3.1. SEM and XRD Analyses. SEM and XRD results indicate that the less miscible, arc-fabricated, brown powders are made of pure Cu Nps, which appear as face-centered cubic (fcc) crystals (Figures 1(a)–1(g) and 2). These SEM images are in contrast to those of the starting copper electrodes, which indicate no evidence of nanostructure, prior to the arc discharge (Figure 1(h)). The visual inspection of the SEM images shows conspicuous current effects on the yield, size, and morphology of brown Cu Nps (Figure 1). Accordingly, in the distilled water, 50 A is rather the best current which produce the size-selected, single crystalline Cu Nps with the average size of 58 nm (Figure 1(a), see (S), Figure S1in Supplementary Material available online at doi: 10.1155/2010/403197).

SEM results show that increasing the current enlarges mean-sizes of the Cu Nps (Figure S1). Obviously, the higher arc currents increase the rate of anodic erosion, causing an increase in the macroparticle formations [14]. At currents higher than 100 A, the yield of Nps drops while their sizes increase (Figures 1(e)–1(g), Figure S1). This is due to the higher rate of vaporization of copper atoms at higher currents, making the growth rate of particles higher leading to larger particle size [31]. As a result, the sizes of Cu Nps are directly proportional to the currents employed (Figure 3). While changing current has significant effects on the particle size, it does not show any noticeable impact on the Cu Nps compositions. Hence, brown Cu Nps, formed in distilled water, at different currents, show XRD lines (111), (200), and (220) at $2\theta = 43.29^\circ, 50.43^\circ, 74.10^\circ$, respectively (Figure 2).

In other words, at all currents positions and intensities of XRD peaks are similar, suggesting arc fabrications of pure Cu Nps. At all the employed currents, a watery black nanopowder is produced as a byproduct (*w/w* 1 : 50), in addition to the arc fabricated brown Cu Nps (Figure S2). The XRD patterns of the brown Cu Nps, fabricated at different currents, do not change after one-month storages in the open air, or distilled water. In contrast, one month storages of the "black nanopowders", in distilled water, induce changes in their XRD patterns, reflecting further oxidation of Nps (Figure S3b). We obtained merely the brown nanopowder in the arc fabrication experiment using a PVP aqueous medium (w/v 1 : 1), at 50 A [13, 32]. Due to coordination between Cu and PVP, the oxidation of Cu Nps is avoided. Its XRD and SEM results show pure Cu Nps with average grain size of 50 nm, respectively (Figure S4).

3.2. TEM Analysis. Using the current of 50 A (current of choice), TEM images of Cu Nps illustrate their spherical morphologies, confirming the SEM images (Figures 4 and 1(a)). To the best of our knowledge, this is the first report on the arc synthesis of metallic Cu Nps with such a fine particle size. Assuming that an Np is spherical, the average diameter of Nps is estimated to be about 20 nm by averaging the diameters of the 50 particles measured in several directions in the TEM image, which is remarkably different with those primarily estimated through SEM (58 nm) analysis, indicating high precision of TEM apparatus. However, small particles aggregate into second particles because of their extremely small dimensions and high surface energy (Figure 4(a)). The selected-area electron diffraction (SAED) pattern displays that the Nps are multiple-surface orientated consisting mainly of Cu atoms with a face-center cubic (fcc) structure (Figure 4(b)). The three characteristic diffraction rings are made of diffraction spots corresponding to (111), (200), and (220) faces of the fcc Cu crystal from the inside to the outside diffraction ring, respectively. This result confirms XRD findings (Figure 2).

3.3. TGA-DTA Analysis. Decomposition kinetics and thermal stabilities are deduced through TGA-DTA, on 5 mg samples of the preheated Cu Nps (arc fabricated at 50 A, as the best current) (Figure 5). Rather rapid weight decrease is observed at 25–100°C, due to vaporization of the residual

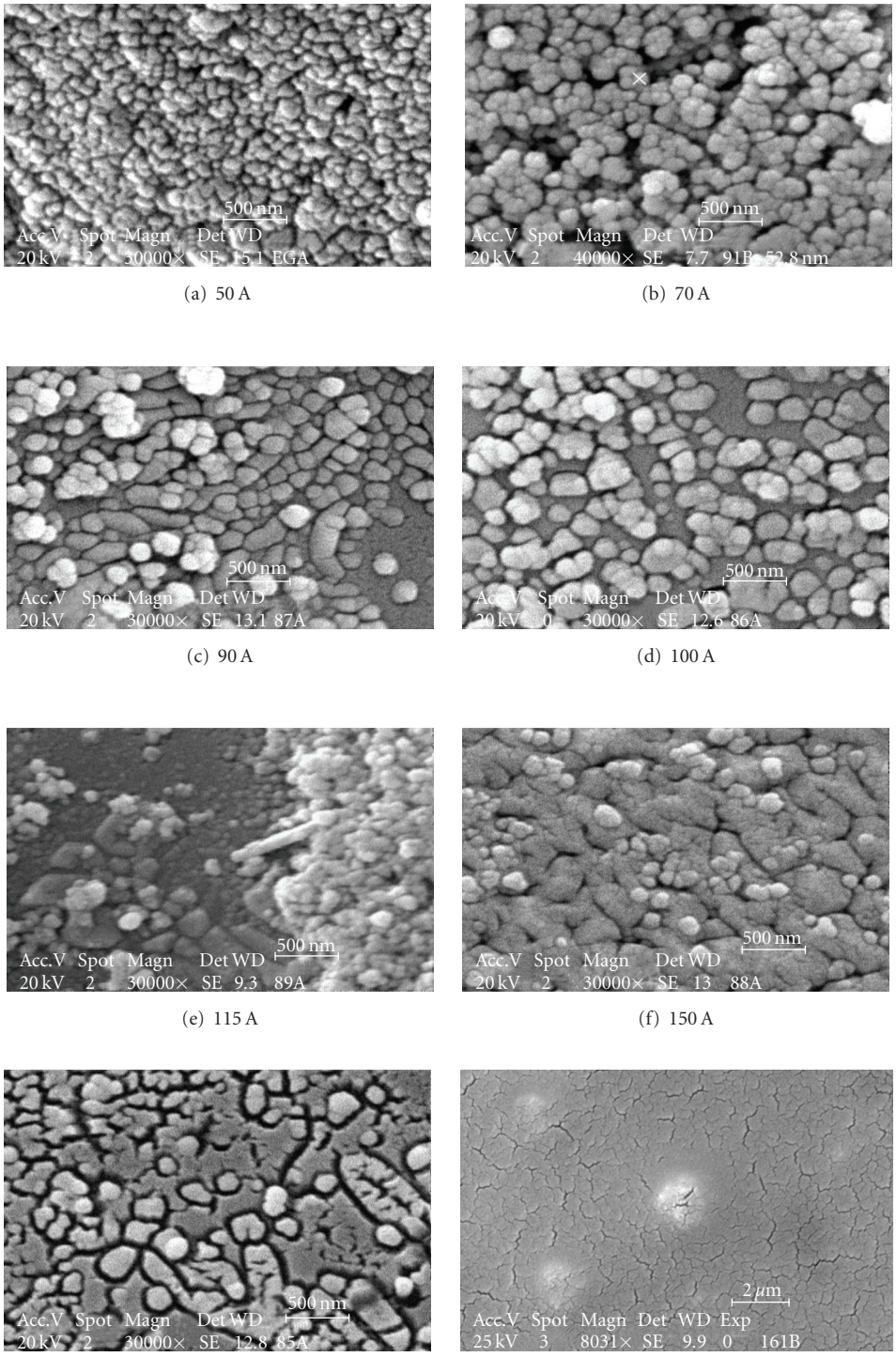

(a) 50 A (b) 70 A

(c) 90 A (d) 100 A

(e) 115 A (f) 150 A

(g) 160 A (h) The starting copper electrode

Figure 1: SEM images showing the effects of seven different currents (50–160 A) on the arc fabricated brown copper nanoparticles, Cu Nps (a)–(g), along with the starting copper rod image, prior to the arc discharge (h).

water contents, with weight losses of about 0.4%, showing small exothermic peak on DTA. No significant weight loss is observed in the range of 100–400°C, where the weight remains constant, indicating no quantitative oxidation behavior of Cu Nps by TGA-DTA. This result shows thermal stability of the Cu Nps in distilled water at 50 A. The decomposition of particles begins at 410°C (weight regular decrease onTGA curve, Figure 5).

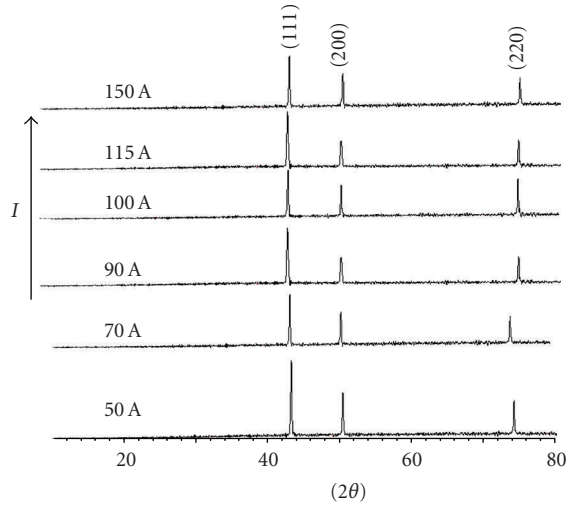

Figure 2: XRD patterns of arc fabricated Cu Nps, as-produced in distilled water, at different currents (50–150 A).

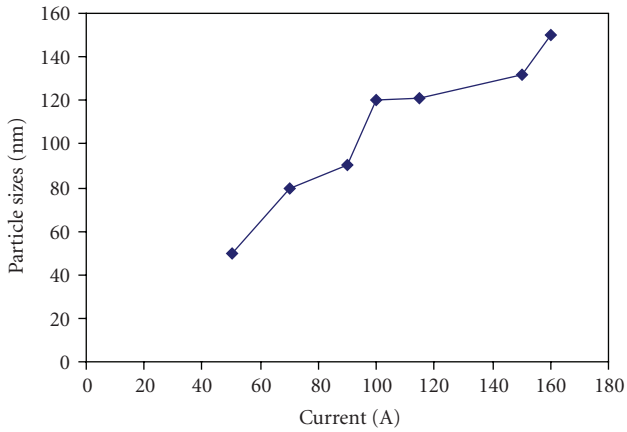

Figure 3: Variation of as-produced Cu Nps sizes as a function of employed currents (50–160 A).

4. Conclusion

Cu Nps are prepared in a large scale arc discharging with homemade apparatus at different currents (50–160 A). Density of current is found as a key factor for the morphology, controlling particle sizes, and yields of Cu Nps. It is found that decreasing the current results in a substantial decrease in the particle size. According to SEM results, the trend of Cu Nps size is proportional to working current showing 50 A (58 ± 9 nm) > 70 A (74 ± 12 nm) > 90 A (97 ± 17 nm) > 100 A (131 ± 20 nm). 50 A appear the best current for fabrication of pure, small, and high yield of Cu Nps. The TEM images show that the Cu Nps are spherical with a narrow particle size distribution and an average particle size of 20 nm (58 nm indicated by SEM). Its XRD and SEAD results indicate the fcc structure of synthesized Cu Nps. Changing current has significant effects on the particle size, while it does not show impact on the Cu Nps compositions.

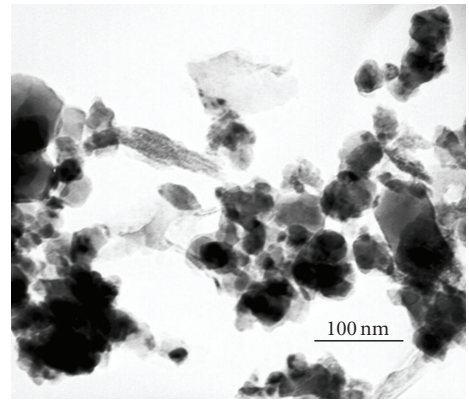

(a)

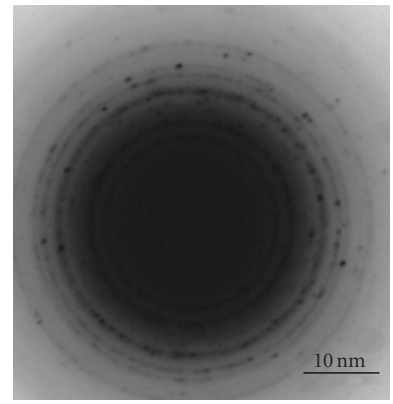

(b)

Figure 4: TEM image (a) and the selected-area electron diffraction pattern (b), of Cu Nps synthesized by arc discharge in distilled water, at 50 A.

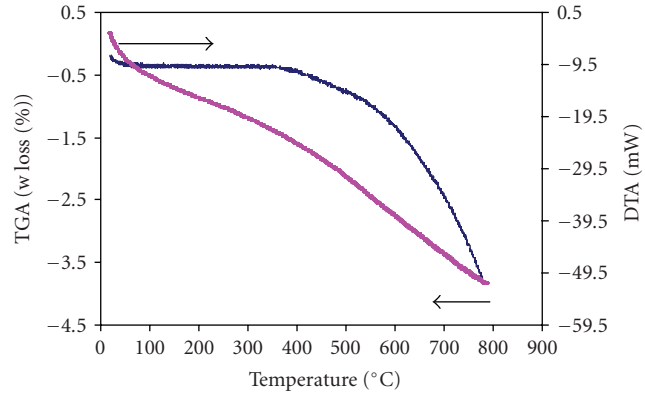

Figure 5: TGA-DTA plots of Cu Nps arc fabrication of 50 A, in distilled water, at a 20–800°C range with a rate of 10°C /min, using air atmosphere.

Acknowledgment

The authors wish to thank Mr. Rezaee (SEM) and Mrs. Fardindost (XRD) for their support. The authors gratefully acknowledge the Iran Nanotechnology Initiative Council (INIC) for financial support.

References

[1] S.-J. Park, A. A. Lazarides, C. A. Mirkin, and R. L. Letsinger, "Directed assembly of periodic materials from protein and oligonucleotide-modified nanoparticle building blocks," *Angewandte Chemie International Edition*, vol. 40, no. 15, pp. 2909–2912, 2001.

[2] Z. Liu, Y. Yang, J. Liang, et al., "Synthesis of copper nanowires via a complex-surfactant-assisted hydrothermal reduction process," *Journal of Physical Chemistry B*, vol. 107, no. 46, pp. 12658–12661, 2003.

[3] R. S. Rao, A. B. Walters, and M. A. Vannice, "Influence of crystallite size on acetone hydrogrnation over copper catalysts," *Journal of Physical Chemistry B*, vol. 109, no. 6, pp. 2086–2092, 2005.

[4] A. A. Ponce and K. J. Klabunde, "Chemical and catalytic activity of copper nanoparticles prepared via metal vapor synthesis," *Journal of Molecular Catalysis A*, vol. 225, no. 1, pp. 1–6, 2005.

[5] S. Cai, X. Xia, and C. Xie, "Research on Cu^{2+} transformations of Cu and its oxides particles with different sizes in the simulated uterine solution," *Corrosion Science*, vol. 47, no. 4, pp. 1039–1047, 2005.

[6] N. D. Nikolic, K. I. Popov, L. J. Pavlovic, and M. G. Pavlovic, "Morphologies of copper deposits obtained by the electrodeposition at high overpotentials," *Surface and Coatings Technology*, vol. 201, no. 3-4, pp. 560–566, 2006.

[7] A. J. Atanacio, B. A. Latella, C. J. Barbé, and M. V. Swain, "Mechanical properties and adhesion characteristics of hybrid sol-gel thin films," *Surface and Coatings Technology*, vol. 192, no. 2-3, pp. 354–364, 2005.

[8] J. P. Cason, M. E. Miller, J. B. Thompson, and C. B. Roberts, "Solvent effects on copper nanoparticle growth behavior in AOT reverse micelle systems," *Journal of Physical Chemistry B*, vol. 105, no. 12, pp. 2297–2302, 2001.

[9] S.-H. Wu and D.-H. Chen, "Synthesis of high-concentration Cu nanoparticles in aqueous CTAB solutions," *Journal of Colloid and Interface Science*, vol. 273, no. 1, pp. 165–169, 2004.

[10] H. Zhu, C. Zhang, and Y. Yin, "Novel synthesis of copper nanoparticles: influence of the synthesis conditions on the particle size," *Nanotechnology*, vol. 16, no. 12, pp. 3079–3083, 2005.

[11] E. Lester, P. Blood, J. Denyer, D. Giddings, B. Azzopardi, and M. Poliakoff, "Reaction engineering: the supercritical water hydrothermal synthesis of nano-particles," *Journal of Supercritical Fluids*, vol. 37, no. 2, pp. 209–214, 2006.

[12] W. Hu, L. Zhu, D. Dong, W. He, X. Tang, and X. Liu, "Thermal behavior of copper powder prepared by hydrothermal treatment," *Journal of Materials Science*, vol. 18, no. 8, pp. 817–821, 2007.

[13] M. Chandra, S. S. Indi, and P. K. Das, "First hyperpolarizabilities of unprotected and polymer protected copper nanoparticles prepared by laser ablation," *Chemical Physics Letters*, vol. 422, no. 1–3, pp. 262–266, 2006.

[14] C. Qin and S. Coulombe, "Organic layer-coated metal nanoparticles prepared by a combined arc evaporation/condensation and plasma polymerization process," *Plasma Sources Science and Technology*, vol. 16, no. 2, pp. 240–249, 2007.

[15] T.-T. Tsung, H. Chang, L.-C. Chen, L.-L. Han, C.-H. Lo, and M.-K. Liu, "Development of pressure control technique of an arc-submerged nanoparticle synthesis system (ASNSS) for copper nanoparticle fabrication," *Materials Transactions*, vol. 44, no. 6, pp. 1138–1142, 2003.

[16] C.-H. Lo, T.-T. Tsung, and L.-C. Chen, "Shape-controlled synthesis of Cu-based nanofluid using submerged arc nanoparticle synthesis system (SANSS)," *Journal of Crystal Growth*, vol. 277, no. 1–4, pp. 636–642, 2005.

[17] C.-H. Lo, T.-T. Tsung, L.-C. Chen, C.-H. Su, and H.-M. Lin, "Fabrication of copper oxide nanofluid using submerged arc nanoparticle synthesis system (SANSS)," *Journal of Nanoparticle Research*, vol. 7, no. 2-3, pp. 313–320, 2005.

[18] H. Chang, C. S. Jwo, C. H. Lo, T. T. Tsung, M. J. Kao, and H. M. Lin, "Rheology of CuO nanoparticle suspension prepared by ASNSS," *Reviews on Advanced Materials Science*, vol. 10, no. 2, pp. 128–132, 2005.

[19] C.-H. Lo, T.-T. Tsung, and L.-C. Chen, "Fabrication and characterization of CuO nanorods by a submerged arc nanoparticle synthesis system," *Journal of Vacuum Science and Technology B*, vol. 23, no. 6, pp. 2394–2397, 2005.

[20] M.-J. Kao, C.-H. Lo, T.-T. Tsung, and H.-M. Lin, "Development of pressure technique of brake nanofluids from an arc spray nanoparticles synthesis system," *Materials Science Forum*, vol. 505–507, no. 1, pp. 49–54, 2006.

[21] M. J. Kao, C. H. Lo, T. T. Tsung, Y. Y. Wu, C. S. Jwo, and H. M. Lin, "Copper-oxide brake nanofluid manufactured using arc-submerged nanoparticle synthesis system," *Journal of Alloys and Compounds*, vol. 434-435, pp. 672–674, 2007.

[22] W.-T. Yao, S.-H. Yu, Y. Zhou, et al., "Formation of uniform CuO nanorods by spontaneous aggregation: selective synthesis of CuO, Cu_2O, and Cu nanoparticles by a solid-liquid phase arc discharge process," *Journal of Physical Chemistry B*, vol. 109, no. 29, pp. 14011–14016, 2005.

[23] C.-H. Lo, T.-T. Tsung, and H.-M. Lin, "Preparation of silver nanofluid by the submerged arc nanoparticle synthesis system (SANSS)," *Journal of Alloys and Compounds*, vol. 434-435, pp. 659–662, 2007.

[24] C.-H. Lo, T.-T. Tsung, and L.-C. Chen, "Ni nano-magnetic fluid prepared by submerged arc nano synthesis system (SANSS)," *JSME International Journal, Series B*, vol. 48, no. 4, pp. 750–755, 2006.

[25] C.-S. Jwo, D.-C. Tien, T.-P. Teng, et al., "Preparation and UV characterization of TiO_2 nanoparticles synthesized by SANSS," *Reviews on Advanced Materials Science*, vol. 10, no. 3, pp. 283–288, 2005.

[26] M. Z. Kassaee, M. Ghavami, and E. Motamedi, "Open air exploding arc synthesis of nano Cu and Cu_2O," *Asian Journal of Chemistry*, vol. 20, no. 1, pp. 677–680, 2008.

[27] M. Z. Kassaee, E. Motamedi, M. Majdi, A. Cheshmehkani, S. Soleimani-Amiri, and F. Buazar, "Media effects on nanobrass arc fabrications," *Journal of Alloys and Compounds*, vol. 453, no. 1-2, pp. 229–232, 2008.

[28] M. Z. Kassaee and F. Buazar, "Al nanoparticles: impact of media and current on the arc fabrication," *Journal of Manufacturing Processes*, vol. 11, no. 1, pp. 31–37, 2009.

[29] J. H. J. Scott and S. A. Majetich, "Morphology, structure, and growth of nanoparticles produced in a carbon arc," *Physical Review B*, vol. 52, no. 17, pp. 12564–12571, 1995.

[30] M. R. Patel, M. A. Barrufet, P. T. Eubank, and D. D. DiBitonto, "Theoretical models of the electrical discharge machining process. II. The anode erosion model," *Journal of Applied Physics*, vol. 66, no. 9, pp. 4104–4111, 1989.

[31] V. I. Levitas, B. W. Asay, S. F. Son, and M. Pantoya, "Melt dispersion mechanism for fast reaction of nanothermites," *Applied Physics Letters*, vol. 89, no. 7, Article ID 071909, 2006.

[32] Y. Wang, P. Chen, and M. Liu, "Synthesis of well-defined copper nanocubes by a one-pot solution process," *Nanotechnology*, vol. 17, no. 24, pp. 6000–6006, 2006.